Plasmons in cuprate superconductors

Ivan Bozovic
Varian Research Center, 611 Hansen Way, Palo Alto, California 94303
(Received 23 October 1989; revised manuscript received 6 April 1990)

The customary way of determining the complex dielectric constant from the measured reflectance spectra suffers from large uncertainties because of the extrapolations required for the Kramers-Kronig transformation. To avoid these, a method is introduced in which reflectance and ellipsometric data on single crystals and epitaxial films are combined. Utilizing this approach, the spectral functions of $YBa_2Cu_3O_7$ (Y-Ba-Cu-O) and $Bi_2Sr_2CaCu_2O_8$ (Bi-Sr-Ca-Cu-O) are determined with substantially improved accuracy. This enables the unambiguous identification of optic plasmons at 1.4 eV in Y-Ba-Cu-O and at 1.1 eV in Bi-Sr-Ca-Cu-O. No other low-lying optic plasmons are detected, which likely rules out most plasmon-mediated superconductivity models. Next, the bare plasma frequency is found to be $\hbar\omega_p = 3.2 \pm 0.3$ eV in Y-Ba-Cu-O and $\hbar\omega_p = 2.4 \pm 0.3$ eV in Bi-Sr-Ca-Cu-O. These values support ascribing the strong infrared absorption to charge carriers which, however, are not free-electron-like, but rather show characteristic polaronic behavior. Finally, in both Y-Ba-Cu-O and Bi-Sr-Ca-Cu-O, it is found that $\mathrm{Im}(-1/\epsilon) = \beta\omega^2$ for small ω, and this law is conjectured to be universal for all layered cuprate superconductors. It is again not Drude-like; it may be compatible with the layered electron-gas model. The latter implies existence of a broad band of acoustic plasmon branches.

I. INTRODUCTION

A. Low-energy excitations and high-temperature superconductivity

Discovery of high-temperature superconductivity (HTSC) in certain copper oxide compounds has triggered an unprecedented world-wide research activity.[1-3] While certainly there are many important technological issues involved, the paramount scientific problem is, undoubtedly, to understand what makes some of these compounds superconducting at temperatures as high as 125 K and perhaps even higher. Addressing this question, a vast number of theoretical models have already been proposed (see Refs. 2 and 3 and references therein), but very few of those have been worked out in enough detail to provide specific, experimentally refutable predictions. Yet, these models vary widely in the basic assumptions made about the nature of the charge carriers (ordinary band electrons, holons, bipolarons, . . .) and/or the bosonic excitations (phonons, excitons, magnons, plasmons, . . .) assumed to mediate the pairing interaction. It is in this context that an experimental study of low-energy excitations in the cuprates could perhaps be relevant for deciphering the mechanism of HTSC. (By "low energy," we mean less than about 2 eV; this is a natural cutoff provided by the optical gap of the "parent" insulating compounds such as La_2CuO_4 and $YBa_2Cu_3O_6$.)

With this motivation, we have undertaken an extensive and systematic study of optical properties of various members of the HTSC-cuprate family. A range of methods (reflectance and Kramers-Kronig transformation; reflectance and transmittance of a thin film; transmittance through several films of different thicknesses; reflectance and ellipsometry) has been investigated comparatively. The method finally chosen and the optical constants obtained we believe to be accurate and reliable. Both are presented in the following, together with a discussion of the character of plasmons and the value of plasma frequency in materials under study. The latter is an important input parameter for a discussion of the nature of charge carriers. This will be presented in the sequel,[4] where an analysis of the dependence of the spectra on temperature and carrier concentration is given.

B. Plasmons and HTSC

The motivation to study plasmons in cuprate superconductors is twofold. First, plasmons mediate the pairing interaction in several theoretical models. However, even among these authors there is much agreement about the specific nature of plasmons involved. For example, Ruvalds[5] has postulated two types of charge carriers (heavy and light), with two corresponding plasmons (at about 0.1 eV and at about 1 eV, respectively). Griffin[6] has assumed the existence of an acoustic plasmon branch originating from out-of-phase charge fluctuations on CuO_2 sheets and CuO chains in Y-Ba-Cu-O. In Gersten's model,[7] two-dimensional (2D) ionic and electronic plasmon modes are coupled, giving rise to a normal, higher-energy, electron-plasmon-like mode and a highly anomalous, soft acoustic mode which does not rise above about 1 meV or so. Kresin and Morawitz[8] have put forward a layered electron-gas model with a whole band of acousticlike plasmon branches. Ashkenazi, *et al.*[9] propose that low-frequency, "heavy axis" plasmons are involved, etc.

Second, the plasma frequency—defined by $\omega_p^2 = 4\pi Ne^2/m^*$, where N is the charge carrier concen-

tration and m^* is the *optical* effective mass—is one of the key electronic parameters needed to characterize the normal state of metallic cuprates, the nature of which is still controversial. (Note that "plasma frequency" is somewhat of a misnomer: ω_p is *not* the frequency of plasmons in real materials. A better approximation, in particular for good metals, is the *screened plasma frequency* $\tilde{\omega}_p \approx \omega_p / \sqrt{\epsilon_\infty}$, where ϵ_∞ is the "background" dielectric constant. The two are often confused, and to avoid that we exclusively refer to ω_p in what follows.)

Attempts to determine the plasma frequency in cuprates have been numerous.[10–50] Let us focus on $YBa_2Cu_3O_7$ (Y-Ba-Cu-O) first, since this compound has been studied most extensively and presumably is best understood from the materials science point of view. In Table I, we have listed the values of $\hbar\omega_p$ reported so far for Y-Ba-Cu-O. Apparently, they are scattered enormously over several orders of magnitude. The discrepancy can be somewhat reduced by discarding the highest few values; these come from electron energy loss spectroscopy (EELS) studies, and they actually correspond to "valence-electron" or "bound-electron" plasmons which cannot be relevant for superconductivity. (This does *not* mean that the data of Refs. 44–46 are in error, but merely that in what follows we refer to free charge carrier plasmons, which are of some potential interest as candidate bosonic excitations.) Still, a large discrepancy remains; it partly originates from certain material-related difficulties which have been understood since.

As for $Bi_2Sr_2CaCu_2O_8$ (Bi-Sr-Ca-Cu-O), the reports on ω_p are still comparatively scarce; yet, the values are already spread out over more than an order of magnitude, indicating that some problems transcend the materials differences and may well be of methodological character.

In the rest of this section, we try to identify the principal causes of uncertainty about ω_p; in Sec. II, we present an attempt to considerably improve the accuracy in determining the spectral functions of cuprate superconductors.

C. Material-related problems

1. *Reflectance*

Early studies of reflectance from pressed-powder pellets were plagued by rough pellet surfaces formed of irregular, highly anisotropic yet randomly oriented grains, by oxygen-depleted surface regions formed as a result of inadequate sample handling, and quite likely by the presence of some insulating phases; the overall result was generally very low reflectance. For this reason, we may also discard the lowest few ω_p values in Table I. Still, a few

TABLE I. The plasma frequency of Y-Ba-Cu-O for electrons moving parallel to CuO_2 layers, $\omega_p^{\parallel}$, and perpendicular to CuO_2 layers, $\omega_p^{\perp}$, P=powder or pressed pellet; F=thin film; C=crystal; M=mosaic of small crystals; Ca (Cb)=monodomain crystal, field along a axis (b axis); FIR=far infrared reflectance; IR=infrared reflectance; IR/UV=infrared through far ultraviolet reflectance; IRT=infrared reflectance and transmittance; μw=microwave measurements; μSR=muon spin resonance; χ=magnetic susceptibility measurements; KI=kinetic inductance measurements; EELS=electron-energy loss spectroscopy; ell=ellipsometry; NR=spin-polarized neutron reflection. Note that in Refs. 12, 14, 19, 22–24, 26–30, and 43 the magnetic penetration depth was reported actually; the values of plasma frequency listed here are obtained using $\hbar\omega_p = hc/\lambda(0)$.

I	$\hbar\omega_p^{\parallel}$ (eV)		0.06–0.15	0.17	0.32	0.5	0.52	0.5–1	0.74	0.75–0.95		
II	Reference		10	11	12	13	14	15	16	17		
III	Sample		*P*	*P*	*D*	*P*	*P*	*P*	*P*	*P*		
IV	Method		FIR	FIR	χ	FIR	μw	FIR	IR	IR		
I	0.8	0.87	0.88	0.92	1–1.3	1.2	1.2–1.5	1.25	1.3	1.32		
II	18	19	20	21	22	16	23	24	25	26		
III	*P*	*P*	*P*	Ca	*P*	*M*	*P*	*P*	*M*	*F*		
IV	IR	μSR	IR	IR	μSR	IR	χ	μSR	FIR	KI		
I	1.34	1.34	1.40	1.41	1.86	2.1	2.6	2.6	2.6	2.7	2.7	2.75
II	27	28	29	30	21	31	32	33	34	35	36	37
III	*C*	*P*	*C*	*P*	*Cb*	*P*	*P*	*P*	*F*	*M*	*C,F*	*P*
IV	χ	μSR	μSR	μSR	IR	IR	FIR	IR	IRT	IR	IR	EELS
I	3	3.1	3.1	3.2	4.3	8.8	17	20	25			
II	38	39	40	41	42	43	44	45	44–46			
III	*P*	*C*	*C*	*C*	*P*	*P*	*P*	*P*	*P,C*			
IV	IR	IR/UV	IR	IR	ell	NR	EELS	EELS	EELS			
I	$\hbar\omega p^{\perp}$ (eV)		0.12–0.24		0.23–0.30		<0.28	0.3–0.4				
II	Reference		17		23		29	47				
III	Sample		*P*		*P*		*C*	*C*				
IV	Method		IR		χ		μSR	IR				

hundred percent uncertainty remains, even if we restrict ourselves to reflectance studies on single crystals and highly oriented thin films. With rare exceptions, these were limited to the geometry in which the light beam impinges on the *ab* face of the crystal at a nearly normal incidence. Twinning in Y-Ba-Cu-O "single" crystals and the mosaic structure of epitaxial films wash out possible differences between [100] and [010] directions; hence, in what follows we assume the electric-field vector to be parallel to the CuO_2 layers and discuss plasmons of that polarization.

Thin films are much easier to oxygenate uniformly, and good superconducting Y-Ba-Cu-O films have been grown by many groups. Films with low normal-state resistivity ($\rho \approx 200-300$ $\mu\Omega$ cm at room temperature), with $T_c > 90$ K and 1–2 degrees wide superconducting transitions, with critical currents in excess of 10^7 A/cm^2 at $T=4.2$ K, etc. have been available at Stanford[51] early in 1987. Many of those looked shiny and optically homogeneous, promising good spectroscopic results. Yet their reflectance spectra showed large sample-to-sample variations. An extreme example of this is shown in Fig. 1, where infrared reflectance spectra of four films from the same batch (i.e., grown simultaneously one next to another) are compared. Subsequent investigation showed such variations to be largely surface related. In Fig. 2, we show again the spectra of the "worst" film *D*, from which the top 100-nm-thick layer has been removed several times, sequentially, by ion milling. After a few sputtering sequences, the reflectance of the film *D* reached and even surpassed that of the "best" film *A*, and even that of most Y-Ba-Cu-O single crystals studied by ourselves or described in reports of other groups. A word of caution may be in order here: ion milling itself produces some

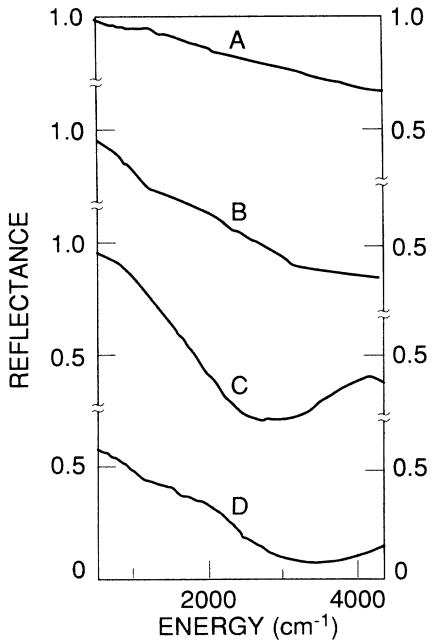

FIG. 1. Sample-to-sample variations in mid-infrared reflectance of four superconducting Y-Ba-Cu-O films, (*A*)–(*D*), from the same batch.

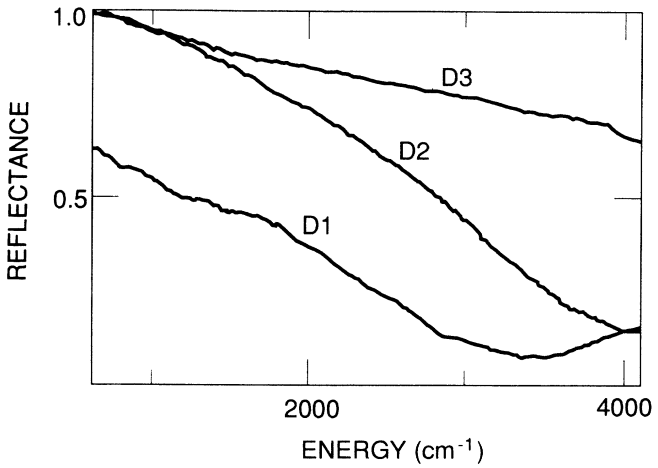

FIG. 2. The effect of surface cleaning on reflectance of a Y-Ba-Cu-O film as grown (*D*1); after the surface layer, 100 nm thick was removed by ion milling (*D*2); with top 200 nm layer removed (*D*3).

surface damage, in general. Very cautious work was done here by Dr. K. Char (who also grew the films *A*–*D*); the ion-beam energy was kept to a minimum, a nearly grazing angle of incidence was employed, and in each milling sequence the last 20 nm were sputtered away by O_2^+ ions to avoid possible oxygen depletion at the surface.[51] Finally, we always recorded the diffuse reflectance spectra; this does not seem to be a common practice and yet in our experience without this check the specular reflectance data can be misleading. Namely, the diffuse reflectance was found to be negligible—evidencing of high surface quality—only in the best few samples. In most films this was not true; the specular reflectance was diminished by surface roughness, and therefore not truly representative of the intrinsic dielectric response of the material.

Single crystals of Y-Ba-Cu-O also require substantial care in sample handling and surface preparation. Addressing this issue, the Princeton group concluded[52] that even a brief exposure of Y-Ba-Cu-O crystals to air results in formation of thick, Y- and O-depleted layer on the surface. Ion milling was found to be beneficial, increasing the reflectance significantly (by 5% or more); their improved spectrum is almost indistinguishable from those of our best cleaned thin films.

Finally, let us mention that the occurrence of stacking faults—such as extra Cu-O layers, for example—is quite common in Y-Ba-Cu-O, in particular in thin films. (In the extreme case, one gets[53] a pure 2:4:8 phase, $Y_2Ba_4Cu_8O_{16}$, which tends to have higher concentrations of charge carriers, higher conductivity and higher reflectance than the 1:2:3 phase.) In Bi-Sr-Ca-Cu-O, stacking faults—e.g., the inclusions of the 2:2:0:1 or the 2:2:2:3 phase—are at least as common.

2. *Transmittance*

Surface-related problems can be largely suppressed by measuring transmittance rather than reflectance. A popular approach is to disperse powder under study in KBr

or to enclose it in polyethylene; however, the problem here is that the optical penetration depth in Y-Ba-Cu-O is less than 100 nm, while the grain size is typically ~ 10 μm or so. Hence, the grains simply *do not transmit* light; it can only leak through by bouncing off grain surfaces. Thus the conclusions based on dispersed-powder transmittance measurements should be assessed carefully. [The same caveat applies to numerous reports of absence of fast (nonbolometric) response to laser pulse excitations based on measurements on pressed pellets or thick films: If the sample is much thicker than the optical penetration depth—i.e., if it is not transparent—the unperturbed, superconducting bottom layer shorts out the signal.]

Real transmittance can be measured conveniently on films a few tens to a few hundred nm thick. Indeed, the first such measurement[34] immediately established an important fact that there are no low-frequency excitons intrinsic to Y-Ba-Cu-O. (Films of various orientations were employed, and a complementary Raman scattering study was performed also in order to eliminate other possible symmetries[34].) The key inference is that the excitonic mechanism of HTSC—at least for the commonly accepted meaning of "exciton" and for the materials known at present—is indeed quite unlikely.

It may be relevant to point out here that transmittance data on Y-Ba-Cu-O also show some, although certainly less striking, sample-to-sample variations. This is illustrated in Fig. 3; notice that some (but not all) films show a feature at about 0.5 eV, *albeit* a very broad and weak one. A similar feature was observed also by Geserich, *et al.*;[54] by plotting $1/T$ rather than T and choosing a favorable scale, they blew up this feature, ascribed it to a *d-d* exciton, and speculated that it may be responsible for the HTSC phenomenon. However, it is shown in Fig. 3 that transmittance spectra of at least some films of excellent superconducting characteristics (high T_c, sharp transitions, high j_c, etc.) do not show any structure near 0.5 eV. Nor did we see the simple correlation between the strength of this feature and the film thickness which was suggested in Refs. 54 and 55; the transmittance inflection at ~ 0.5 eV was quite noticeable in a few rather thin ($d = 50$ nm) films, and it was clearly absent in some much thicker ($d > 400$ nm) ones. Rather, the relevant variable is the carrier concentration; the feature is more pronounced in oxygen-depleted samples.

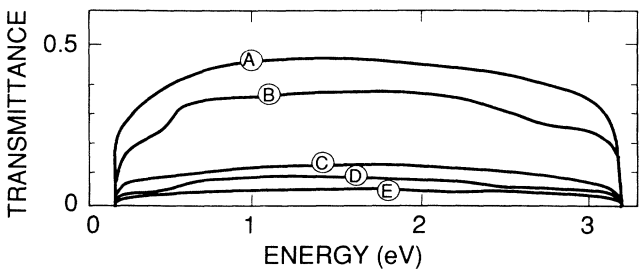

FIG. 3. Sample-to-sample variations in transmittance spectra of Y-Ba-Cu-O films, approximately 50, 70, 180, 200, and 300 nm thick (*A*)–(*E*). Notice appearance of weak features in films *B* and *D*, apparently without correlation to the film thickness.

The origin of the preceding discrepancy is in all likelihood materials related again. Namely, all HTSC thin films produced so far have been granular, with some fraction (at least a few percent in the very best samples and typically more) of grains misoriented, oxygen depleted, of a wrong stoichiometry, etc. Such grains generally transmit light much better than the "good," highly conducting grains aligned with the *c* axis perpendicular to the substrate. Knowing as we do now that the transmittance of say a 400-nm thick film should be well below 1%, one must beware of the presence of even a small fraction (say 1%) of insulating grains, which act like windows and could easily dominate the transmittance. Indeed (a) Geserich *et al.* explicitly stated that the 0.5 eV feature is seen clearly only in such thick films, (b) their spectra show a strong 1.7 eV feature known now to be characteristic[56] of oxygen-depleted Y-Ba-Cu-O, (c) the transmittance reported was much too high for the nominal film thickness, and (d) the films were grown on unoriented sapphire, and to our best knowledge such films have so far been inferior to those grown epitaxially on (100) faces of $SrTiO_3$ (Sr-Ti-O) single crystals. All of these are consistent with the preceding interpretation.

One concludes then that transmittance measurements on thinner (say 50–100 nm thick) films should provide more reliable information on the intrinsic optical properties of Y-Ba-Cu-O. If the measured T is, say, about 50% or so, it cannot be affected much by the presence of, say, few percent of "bad," transparent grains. However, even though the general shape of such spectra should be correct, caution is still needed if quantitative determination of optical constants is to be attempted; one should beware of reduced density of the material, pinholes, film/substrate interdiffusion, etc.

The bottom line is that Y-Ba-Cu-O is a complex material; to derive reliable conclusions from optical studies, detailed material characterization, very careful sample handling and study of a large number of samples prepared under different conditions, are all necessary.

Fortunately, the more recent $Bi_2Sr_2CaCu_2O_8$ (Bi-Sr-Ca-Cu-O) compound with $T_c = 85$–90 K is much more forgiving. Large single crystals can be grown; the ones we studied (grown by D. Mitzi at Stanford University[57]) were as large as $10 \times 10 \times 0.2$ mm^3. The material does not lose oxygen readily, in contrast to Y-Ba-Cu-O. Finally, the crystals are cleaved easily, which we did with a pair of vacuum aspirators to avoid contamination. The cleavage generally occurs along the BiO layers (parallel to the *ab* plane) and it produces surfaces almost atomically perfect, as evidenced by scanning tunneling microscope pictures obtained by Kirk *et al.*[58] on some samples from the same batch. These are excellent circumstances for reflectance studies; in contrast, transmittance work on thin Bi-Sr-Ca-Cu-O films still faces most of the problems encountered in Y-Ba-Cu-O.

D. Some methodological difficulties

While material-related problems are serious enough, discrepancies shown in Table I originate at least in part from different methods of analysis, with inequivalent assumptions adopted by different groups.

The simplest approach is to fit the measured reflectance $R(\omega)$ using the Drude model. This is routinely done by many groups, and the value of $\hbar\omega_p$ in Y-Ba-Cu-O is generally found to be about 2.5–3 eV, at least for single crystals and oriented films. It is indeed understood that this is only a *crude* estimate of $\hbar\omega_p$, say good to within 20–30 % or so. An exception to this general attitude may perhaps be provided by some papers of Uchida *et al.*[39,59] who tried to apply this (crude) method to a study of fine variations of ω_p that occur when the oxygen content or doping level are changed, to correlate these to variations in T_c, and from that to derive some far-reaching conclusions about the normal and the superconducting state of the cuprates.

On the opposite side, Timusk and Tanner[60] have (rightfully) pointed out that the temperature dependence of the reflectance does not agree with that of the simple Drude model; they argue that the infrared response of Y-Ba-Cu-O and related cuprates is a superposition of a (low-frequency) charge-carrier response and a (higher-frequency) charge-transfer exciton or interband transition. Of principal importance here is that the plasma frequency is necessarily much lower ($\hbar\omega_p = 0.5-1.5$ eV) in such a model. Hence, the spread of values of Tables I and II largely originate from inequivalent methods of extracting ω_p from the experimental data.

Certainly, we agree that the simple Drude model does not describe adequately the physics of cuprate superconductors. Indeed, we have already pointed out[34] that the damping obtained from the fit is large and suggestive of polaron formation or quasilocalization; optically, Y-Ba-Cu-O resembles a heavily-doped polaronic semiconductor much more than a good metal. Polaronic effects are indeed expected[4,61] to modify the infrared response (and its temperature dependence), which nevertheless still *originates from charge carriers.* It is for this physical reason that the Drude model could still provide a reasonable first guess (but nothing better than that) for $\hbar\omega_p$, which we are argue below should actually be close to ~ 3 eV in Y-Ba-Cu-O.

Another popular and in principle model-independent approach is to use the Kramers-Kronig transformation:

$$\theta(\omega)=\frac{\omega}{\pi}\int_0^\infty \frac{\ln R(\omega')-\ln R(\omega)}{\omega^2-\omega'^2}d\omega' \tag{1}$$

to derive the phase $\theta(\omega)$ from the known reflectance spectrum. Once both $R(\omega)$ and $\theta(\omega)$ are known, one can calculate all other optical constants:

$$n=\frac{1-R}{1+R-2\sqrt{R}\cos\theta}\ , \tag{2}$$

$$k=\frac{2\sqrt{R}\sin\theta}{1+R-2\sqrt{R}\cos\theta}\ , \tag{3}$$

$$\epsilon_1=n^2-k^2\ , \tag{4}$$

$$\epsilon_2=2nk\ , \tag{5}$$

$$\mathrm{Re}\sigma=4\pi\epsilon_2/\omega\ , \tag{6}$$

etc. Finally, one can determine ω_p from the sum rule:

$$I(\omega_1)=\int_0^{\omega_1}\mathrm{Re}\sigma(\omega)d\omega=\omega_p^2/8\ , \tag{7}$$

where ω_1 is a certain cutoff frequency, high enough to have the entire free-carrier response included but low enough to exclude all interband transitions. In simple metals, the two spectral ranges are usually well separated; in between them, the integral $I(\omega_1)$ does not vary with ω_1. However, in the case of Y-Ba-Cu-O, $\mathrm{Re}\sigma(\omega)$ is almost featureless (as will be shown later in Sec. IV A), and hence the function $I(\omega_1)$ increases monotonically with ω_1, the choice of which then becomes ambiguous.

An even larger uncertainty is brought in by high-frequency extrapolations for $R(\omega)$ that have been employed so far for Y-Ba-Cu-O. Namely, to calculate accurately the integral in (7), one needs to know the function $R(\omega)$ over the whole spectral region; in practice, this means over a range wide enough to include all significant spectroscopic features. However, most reflectance studies of superconducting cuprates reported so far were restricted to a range between a few meV to a few eV at best, just barely entering the interband transition range. In many cases, only the far-infrared region (few meV to less than 0.1 eV) was studied, but nevertheless the Kramers-Kronig transformation was utilized. Needless to say, one should not trust the optical constants derived under such circumstances.

It may be of interest to predict the sign of the error. Actually, different groups employ different forms of high-frequency extrapolation, but in most cases this turns out to be some fast-decaying function of ω, such as $R(\omega)\sim 1/\omega^2$ for $\omega \geq \omega_2$, or $R(\omega)\sim 1/\omega^2$ for $\omega_2 \leq \omega \leq \omega_3$ and $R(\omega)\sim 1/\omega^4$ for $\omega > \omega_3$ (where ω_2, ω_3 are some cutoff frequencies), etc. In each case, one grossly *underestimates* the strong absorption given rise by interband transitions above 2–3 eV, which in reality do take place in Y-Ba-Cu-O as well as in other HTSC compounds. Given the sum rule (7), one then expects some artificial piling up of the oscillator strength to occur at lower energies. This, in turn, may (artificially) push down the plasma frequency.

In principle, the error margin of the preceding method

TABLE II. The plasma frequency in Bi-Sr-Ca-Cu-O for electrons moving parallel to CuO_2 layers, $\omega_p^{\parallel}$, and perpendicular to CuO_2 layers, $\omega_p^{\perp}$. For abbreviations, see the caption of Table I.

$\hbar\omega_p^{\parallel}$ (eV)	0.25	0.66	0.88	1.44	2.85	$\hbar\omega_p^{\perp}$ (eV)	0.06–0.14
Reference	48	17	48	49	50	Reference	23
Sample	*P*	*C*	*C*	*C*	*C*	Sample	*C*
Method	IR	χ	IR	IR	EELS	Method	χ

could be reduced by extending the reflectance measurement up to much higher energies, as done in Ref. 39. However, for Y-Ba-Cu-O, this is hardly a panacea: far-UV measurements require high vacuum, which is likely to cause oxygen depletion from surface regions; at the same time, the light penetration depth becomes much shorter in far UV, which aggravates the effect.

Alternatively, uncertainties related to the high-frequency part of the Kramers-Kronig interaction (1) can be avoided if the reflectance measurement can be supplemented by an independent determination of another spectroscopic quantity, such as the transmittance through a thin film. This method of determining the optical constants of Y-Ba-Cu-O has been attempted by several groups; we also have tested it extensively, but found it unsatisfactory for the reasons expounded in the following.

Yet another possible approach is to combine transmittance (T) measurements on two thin Y-Ba-Cu-O films of different thicknesses, and to determine n and k from a pair of equations[62] relating T_1 and T_2 to n and k. An advantage here is that one avoids surface-related problems that frequently plague reflectance measurements on Y-Ba-Cu-O. Pursuing this method, we utilized up to four films (50, 100, 200, and 400 nm thick) simultaneously. In this way, n and k are overdetermined and one has up to five additional consistency checks available. Generally, this is a very accurate and reliable method—provided that the films are of identical composition, homogeneous, fully dense, that the surfaces are smooth and that the film thicknesses are known accurately. Regrettably, none of these requirements is satisfied by the state-of-the-art Y-Ba-Cu-O films. The thickness is difficult to measure to better than 10–20% accuracy, typically, due to surface roughness, voids, reduced density, etc. Finally, such films tend to differ from one to another significantly in composition, in oxygen content, distribution and ordering, etc. Strictly speaking, each film represents a somewhat different material; this fact strongly favors methods in which all the measurements are performed on one and the same sample.

Absorption in the substrate is another drawback of transmittance methods. So far, the best Y-Ba-Cu-O films were grown epitaxially on Sr-Ti-O substrates. Above about 1200 cm^{-1} (0.15 eV), Sr-Ti-O is transparent, but at lower frequencies a typical (say, one mm thick) substrate is completely opaque. This does not affect a study of plasmons such as the present one much, but it does prevent one from observing the superconducting gap in the far-infrared transmittance spectrum, for example. Other commonly employed substrates impose similar problems. The exceptions are Si and, to an extent MgO (which is semitransparent below about 300 cm^{-1}), but so far the quality of Y-Ba-Cu-O films grown on such substrates has been inferior.

We conclude that at this stage none of the four methods just described provides the accuracy and reliability needed to address the issues under study with confidence. With this motivation, we turn now to yet another approach, not applied before to HTSC materials, but which appears to be quite satisfactory.

II. THE METHOD: REFLECTANCE COMBINED WITH ELLIPSOMETRY

Spectroellipsometry is one of the most accurate methods of determining the optical constants of reflective materials.[63] It provides both the real and the imaginary part of the dielectric function determined on a wavelength-by-wavelength basis, without having to resort to the Kramers-Kronig transformation (1). For a homogeneous and fully dense material with a clean and smooth surface, one can obtain ϵ_1, ϵ_2 with accuracy of 1% or so. The method has been applied successfully to metals and semiconductors.[63] More recently, spectroellipsometric studies of Y-Ba-Cu-O pellets, single crystals and thin films, have also been reported.[56,65] Important findings include discovery of absorption features characteristic of oxygen-depleted Y-Ba-Cu-O, such as a sharp exciton at about 4.1 eV and a broader feature at about 1.7 eV. Spectroellipsometric measurements were performed also on a number of thin films referred to in this study by D. Aspnes and M. Kelly at Bellcore (Ref. 47 and unpublished). The dielectric response of the best, cleaned, c axis oriented Y-Ba-Cu-O films was found to be nearly the same as that of the single crystals studied in Ref. 62. Regrettably, these ellipsometric data are restricted to the interval $1.5 < \hbar\omega < 6$ eV; the lower-frequency region—i.e., the one which is of principal interest for a study of the HTSC phenomenon—is currently not accessible.

Nevertheless, the higher-frequency ellipsometric data can still play a very useful role: insofar as they are accurate, they provide certain logical checks with which one can test data obtained by other methods. For example, if one performs an independent normal-incidence reflectance measurement, apparently the measured $R(\omega)$ should coincide with the one calculated from the ellipsometric dielectric functions, in the frequency region common to both measurements. Similarly, $\theta(\omega)$ calculated via the Kramers-Kronig formula (1) should coincide with the one corresponding to the ellipsometric ϵ_1, ϵ_2. The methods currently in use ignore (and fail to fulfill, as will be shown in the following) this requirement, which is precisely what we wish to exploit.

Let us assume that $R(\omega)$ is known accurately for all $\omega \leq \omega_H$. [As already pointed out in Sec. I B, we are able now to measure $R(\omega)$ to a few percent accuracy in Bi-Sr-Ca-Cu-O and (albeit with extreme care) in Y-Ba-Cu-O, up to $\hbar\omega_H = 6$ eV or so. More precisely, our data do not go below a few meV, but at these frequencies $R(\omega) \approx 1$ and $\ln R(\omega) \approx 0$, so that the low-frequency extrapolation has practically no effect on the value of the integral in (1) at higher ω_0.] As a first approximation, let us assume next that $R(\omega) = R_H = \text{const}$ for $\omega \geq \omega_H$. In this way, one gets:

$$\theta_{\text{uncorr}}(\omega) = \frac{\omega}{\pi} \int_0^{\omega_H} \frac{\ln R(\omega') - \ln R(\omega)}{\omega^2 - \omega'^2} d\omega' + \frac{\omega}{\pi} \int_{\omega_H}^{\infty} \frac{\ln R_H - \ln R(\omega)}{\omega^2 - \omega'^2} d\omega' . \quad (8)$$

The first of these two integrals can be calculated numeri-

cally using the measured $R(\omega)$. The second can be solved analytically.

$$\frac{\omega}{\pi}\int_{\omega_H}^{\infty}\frac{\ln R_H-\ln R(\omega)}{\omega^2-\omega'^2}d\omega'=\frac{1}{2\pi}\ln\frac{R_H}{R(\omega)}\ln\frac{\omega_H-\omega}{\omega_H+\omega}\ . \tag{9}$$

In this way, one obtains $\theta_{\text{uncorr}}(\omega)$ for all relevant values of ω—here, for each $\omega\le\omega_H$.

Next, we utilize the ellipsometric (i.e., "exact") functions $\epsilon_1(\omega),\epsilon_2(\omega)$ known for $\omega_L\le\omega\le\omega_H$ (in our case $\hbar\omega_L=1.5$ eV and $\hbar\omega_H=6$ eV) to calculate $\theta_{\text{ell}}(\omega)$. On the other hand, the latter equals:

$$\theta_{\text{ell}}(\omega)=\frac{\omega}{\pi}\int_0^{\omega_H}\frac{\ln R(\omega')-\ln R(\omega)}{\omega^2-\omega'^2}d\omega + \frac{\omega}{\pi}\int_{\omega_H}^{\infty}\frac{\ln R(\omega')-\ln R(\omega)}{\omega^2-\omega'^2}d\omega\ , \tag{10}$$

where now we know the left-hand-side function and the first integral; in the second integral, the function $R(\omega)$ appears, which for $\omega>\omega_H$ is not known. We can subtract (9) from (10) to get:

$$\Delta\theta(\omega)=\theta_{\text{ell}}(\omega)-\theta_{\text{uncorr}}(\omega) =\frac{\omega}{\pi}\int_{\omega_H}^{\infty}\frac{\ln R(\omega')-\ln R_H}{\omega^2-\omega'^2}d\omega'\ . \tag{11}$$

Next, we make use of the following:[65] If $g(x)$ is a well-behaved real function, one has

$$\int_a^{\infty}\frac{g(x)dx}{x^2-y^2}=\sum_{n=0}^{\infty}C_n y^{2n}\ , \tag{12}$$

where

$$C_n=\int_a^{\infty}\frac{g(x)dx}{x^{2n+2}}\ . \tag{13}$$

Apparently, the integrand in (11) is of the form required above, and hence we can expand $\Delta\theta(\omega)$ in a power series:

$$\Delta\theta(\omega)=\frac{\omega}{\pi}\sum_{n=0}^{\infty}D_n\omega^{2n}\ , \tag{14}$$

where

$$D_n=-\int_a^{\infty}\frac{\ln R(\omega')-\ln R_H}{\omega'^{2n+2}}d\omega'\ , \tag{15}$$

which furthermore converges rapidly, since

$$|D_{n+1}|=\int_{\omega_H}^{\infty}\left|\frac{\ln R(\omega')-\ln R_H}{\omega'^{2n+4}}\right|d\omega'<\frac{1}{\omega_H^2}|D_n| \tag{16}$$

so that

$$|D_n|<\frac{\text{const}}{\omega_H^{2n}}\ . \tag{17}$$

Hence for all practical purposes, one may approximate $\Delta\theta(\omega)$ quite accurately by a polynomial of not too large a degree—say, five or seven. Our method[66] is shaping up now: (i) measure $R(\omega)$ for $\omega\le\omega_H$, (ii) calculate $\theta_{\text{uncorr}}(\omega)$ by assuming $R(\omega)=R_H$ for $\omega\le\omega_H$, (iii) subtract it from the phase $\theta_{\text{ell}}(\omega)$ derived from ellipsometric data, (iv) fit the function $\Delta\theta(\omega)=\theta_{\text{ell}}(\omega)-\theta_{\text{uncorr}}(\omega)$, in the interval $\omega_L\le\omega\le\omega_H$, by a polynomial

$$\Delta\theta_{\text{poly}}(\omega)=a_1+a_3\omega^3+\cdots+a_{2m+1}\omega^{2m+1} \tag{18}$$

(v) form $\theta_{\text{corr}}(\omega)=\theta_{\text{uncorr}}(\omega)+\Delta\theta_{\text{poly}}(\omega)$ and utilize it to calculate $n(\omega)$ and $k(\omega)$. From those, one can calculate all other spectroscopical functions such as ϵ_1,ϵ_2, the loss function $\text{Im}(-1/\epsilon)$, the absorption coefficient α, the optical penetration depth L, etc.

The accuracy of this method should basically be determined by the accuracy of the ellipsometric measurement and of the normal-incidence reflectance measurement. In the case of cuprate superconductors, we can expect to get ϵ_1,ϵ_2 accurately to within a few percent in the whole frequency range covered, from a few meV to about 6 eV. This accuracy should be quite sufficient for our purpose of identifying the dominant one-electron and collective low-energy excitations in HTSC materials.

III. EXPERIMENTAL

A. Sample preparation and characterization

We have recorded and studied transmittance and reflectance spectra of a few hundred HTSC samples over a period of two years. Most of these were in the form of highly oriented thin films of Y-Ba-Cu-O; a broad range of deposition methods (single- and multiple-target ion sputtering, electron-beam evaporation, molecular-beam epitaxy), growth conditions, substrates, processing protocols, etc. have been employed and compared. Dozens of single crystals have been studied also. Since the details of preparation and characterization procedures have already been described in Refs. 51 and 57, they need not be repeated here. It is sufficient to point out that the samples referred to below were of high quality, ad judged by their x-ray diffraction patterns and electron microprobe analysis which showed the right stoichiometry, by low normal-state resistivity ($\rho\approx200$ $\mu\Omega$ cm for Y-Ba-Cu-O and $\rho\approx100$ $\mu\Omega$ cm for Bi-Sr-Ca-Cu-O at $T=300$ K), by sharp superconducting transitions (1–2 K wide in thin films and less than 0.5 K wide in single crystals), by high critical currents (above 1×10^7 A/cm^2 at 4.2 K in best films), and by mirrorlike surfaces with no defects visible under a microscope. In addition to these structural and transport measurements which were routinely performed, some selected samples (or their neighbors from the same batch) were also characterized by Raman spectroscopy, ellipsometry, x-ray photoelectron spectroscopy, low-energy electron diffraction, scanning tunneling microscopy, Rutherford backscattering spectroscopy, high-resolution transmission electron microscopy, Hall effect, thermopower, tunneling and surface-resistance measurements, etc. In summary, we may assume to have a reasonably detailed knowledge of chemical and crystallographic structure, morphology, etc. of the samples under study.

Various methods of surface cleaning of the sample prior to the spectroscopic work have been explored. As already stated in Sec. II B, we have achieved quite reprodu-

cible results and the highest reflectances by sputtering away thick surface layers by ion milling in the case of Y-Ba-Cu-O, and by vacuum cleaving Bi-Sr-Ca-Cu-O. While the first method does leave some room for improvement, the second satisfies the highest standards and produces virtually perfect surfaces.

B. Measurements

The spectra were recorded on a vacuum far-infrared FTS-40V Digilab Fourier-transform spectrometer, a matching mid-infrared FTS-40 Digilab FTIR spectrometer, and a near-infrared–visible–near-ultraviolet Lambda-9 Perkin-Elmer double-monochromator double-beam spectrophotometer. The mid-IR spectrometer has been coupled to a Spectratech Plan-IR microscope with a dedicated detector, enabling spectroscopic studies of samples as small as 50 μm. The three spectrometers have large spectral overlaps and were found to match one another to about 1%. Under optimal circumstances, absolute accuracy of about 2% and relative accuracy and repeatability of a fraction of a percent were achieved. Harrick diffuse reflectance accessories and a 60-mm integrating sphere with built in photomultiplier and lead-sulfide cell detectors were utilized with the Digilab and the Perkin-Elmer spectrometers, respectively, to measure diffuse reflectance, which was found to be significant in most samples.

C. Results: Reflectance spectra of Y-Ba-Cu-O and Bi-Sr-Ca-Cu-O

Some representative specular near-normal-incidence reflectance spectra of Y-Ba-Cu-O are shown in Fig. 4. They correspond to (*A*) the best Y-Ba-Cu-O thin film oriented with the *c*-axis perpendicular to the substrate, (*B*) a typical *c*-axis Y-Ba-Cu-O film, (*C*) a single crystal of Y-Ba-Cu-O, reflectance measured directly, and (*D*) a single crystal of Y-Ba-Cu-O, reflectance calculated from pseudodielectric functions as determined by ellipsometry.[56] Reflectance spectra of single crystals of Y-Ba-Cu-O have been reported already by several groups. In most cases (with the notable exception of recent high-quality spectra of Watanabe *et al.*[52]), the reflectance was found to be somewhat lower than that of our film (*A*). At the same time, the reported dc conductivities of those single crystals were also lower, by as much as a factor of 2 or 3 in some cases, which could be related to difficulties in achieving complete and homogeneous oxygenation in single-crystal samples.

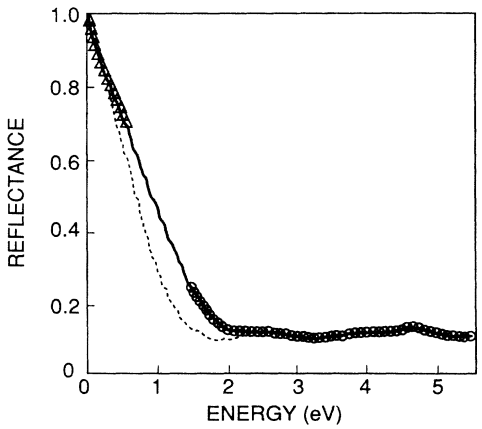

FIG. 4. Broad range specular reflectance spectrum of the best *c* axis oriented Y-Ba-Cu-O film, solid line; of a moderately good Y-Ba-Cu-O film, broken line; from *ab* face of a Y-Ba-Cu-O single crystal, open triangles; and inferred from ellipsometric data (Ref. 56), open circles.

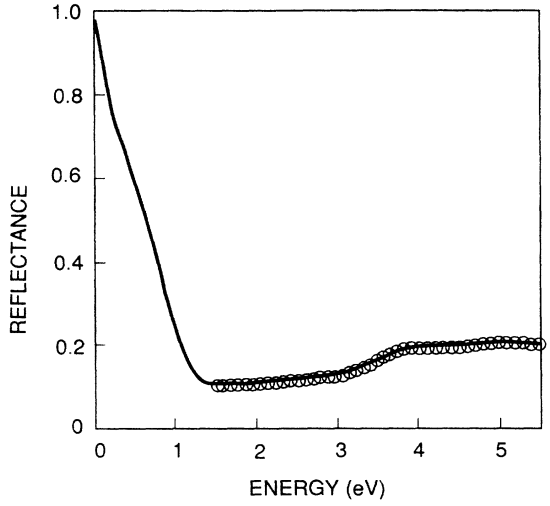

FIG. 5. Broad range specular reflectance from *ab* face of a Bi-Sr-Ca-Cu-O single crystal, solid line; and inferred from ellipsometric data (Ref. 56), open circles.

Notice also the absence of virtually any phonon features in the reflectance spectra of Fig. 4. Together with high reflectivity, this we believe to be a distinguishing characteristic of high quality, high carrier concentration Y-Ba-Cu-O samples which are well oriented with the field perpendicular to *ab* facets; under such circumstances, the in-plane infrared-active phonons are almost entirely screened by free carriers. Deliberate oxygen depletion and/or admixture of *c*-axis reflectance make the phonon features (similar to those commonly observed in inferior samples) reappear.

In Fig. 5, we show a reflectance spectrum of a Bi-Sr-Ca-Cu-O single crystal. Again, it is similar to spectra reported by other groups. The small departures may partly arise from real, material-related differences. They are certainly not sufficient to account for the large discrepancies in the derived values of ω_p; these originate from the different assumptions and methods of analysis.

IV. RESULTS: THE SPECTRAL FUNCTIONS

A. Y-Ba-Cu-O

In Fig. 6, we show three $\theta(\omega)$ functions: (a) the "uncorrected" one, corresponding to the reflectance of film *A* as measured for $\hbar\omega \leq 6$ eV and assumed to have a constant value for $\hbar\omega \geq 6$ eV; (b) the ellipsometric one calculated from ϵ_1, ϵ_2 of Ref. 62; and lastly, (c) the corrected

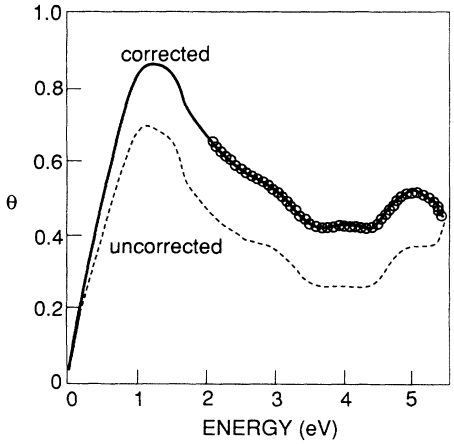

FIG. 6. The phase shift $\Theta(\omega)$ of Y-Ba-Cu-O, calculated assuming R_H=const. for $\hbar\omega \geq 6$ eV, dashed line; from ellipsometric data (Ref. 56), open circles; and utilizing the procedure described in Sec. III, solid line.

one obtained according to the procedure described in the preceding section. The first striking observation is that the correction is large—over 30% in the spectral region 1 eV $<\hbar\omega<2$ eV (where the actual plasmon occurs). It would have been even larger had we employed high-energy extrapolation such as $R(\omega)\sim 1/\omega^2$ or $R(\omega)\sim 1/\omega^4$ (i.e., the ones utilized in most of the recent works), since in that way one assumes much lower reflectances at higher frequencies. The same should be true then for $n,k,\epsilon_1,\epsilon_2,\sigma$. etc., since they all depend on θ as seen from Eqs. (2)–(6). This is illustrated in Fig. 7, where the uncorrected, ellipsometric, and corrected functions ϵ_1,ϵ_2 are shown for comparison. One cannot but conclude that the optical parameters determined via the Kramers-Kronig transformation (1) from the measured reflectance are generally quite uncertain,[67] in spite of the popularity of that approach.

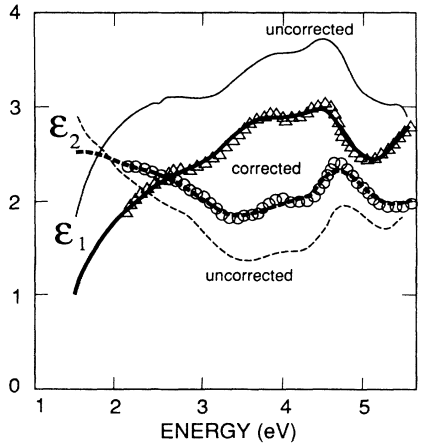

FIG. 7. The real and the imaginary part of the dielectric function $\epsilon=\epsilon_1+i\epsilon_1$ of Y-Ba-Cu-O calculated assuming R_H=const. for $\hbar\omega \geq 6$ eV, thin solid line and thin dashed line, respectively; from ellipsometric data (Ref. 56), open triangles and open circles; and following the procedure described in Sec. III, thick solid line and thick dashed line.

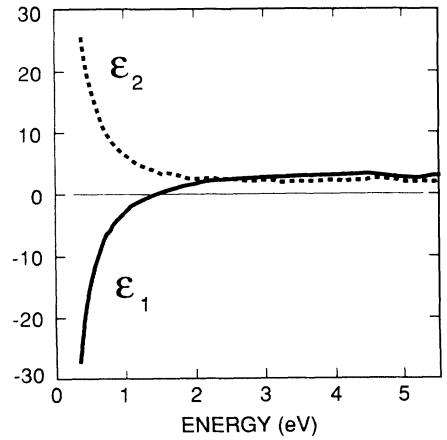

FIG. 8. The real and the imaginary part of the corrected dielectric function of Y-Ba-Cu-O, on an expanded scale.

The corrected ϵ_1,ϵ_2 functions are shown again in Fig. 8 on an extended scale. As the frequency is lowered, ϵ_1 decreases and changes sign at $\hbar\omega=1.4$ eV, and then continues to decrease further, achieving large negative values; indeed, it has no other zeroes in this spectral region. At the same time, ϵ_2 increases from about two to very large positive values, several hundreds at the lowest energies (few meV) covered.

The loss function Im $(-1/\epsilon)$ of Y-Ba-Cu-O is plotted in Fig. 9; it shows a pronounced maximum, also close to 1.4 eV. There are no maxima at lower frequencies.

The real part of the optical conductivity $\sigma(\omega)$ is shown in Fig. 10, and the optical penetration depth $L(\omega)$ is shown in Fig. 11. Notice that Re$\sigma(\omega)$ is quite flat in the region 1 eV $<\hbar\omega<2.5$ eV. Also notice that overall absorption is strong (albeit almost featureless) throughout the infrared, so that the penetration depth is quite short, not longer than several hundred angstroms. Indeed, typical sharp bosoniclike features are not seen[68] in Fig. 10.

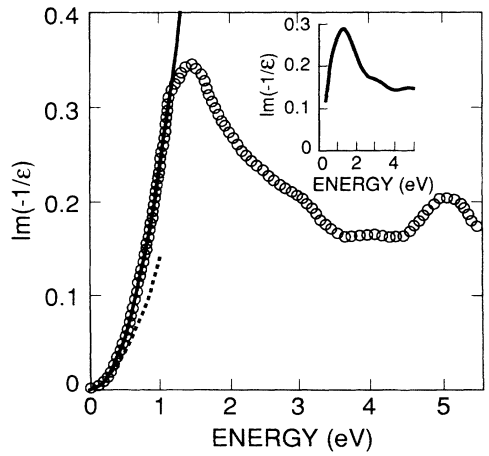

FIG. 9. The loss function of Y-Ba-Cu-O derived in this work (open circles) and from EELS data (Ref. 37) (inset). The solid line shows a square-law fit, Im$(-1/\epsilon)=\beta\omega^2$, and the dashed line is a Drude-law fit (see the text) for $\hbar\omega \leq 1$ eV.

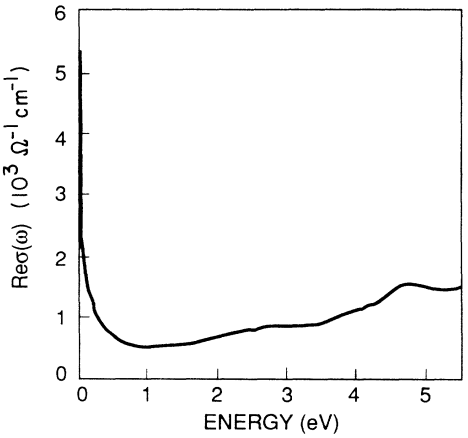

FIG. 10. The real part of the optical conductivity of Y-Ba-Cu-O.

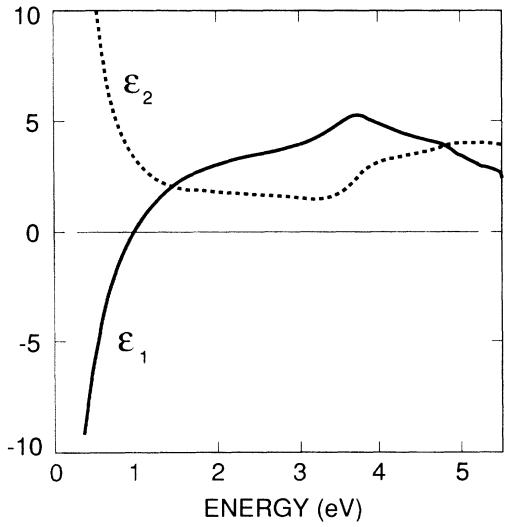

FIG. 12. The real and the imaginary part of the dielectric function of Bi-Sr-Ca-Cu-O.

B. Bi-Sr-Ca-Cu-O

The corrected ϵ_1, ϵ_2 functions are plotted in Fig. 12 for a single crystal of Bi-Sr-Ca-Cu-O. A zero of ϵ_1 is found at $\hbar\omega = 1.0$ eV. The loss function $\mathrm{Im}(-1/\epsilon)$ shown in Fig. 13 has a maximum at about 1.1 eV. Finally, $\mathrm{Re}\sigma(\omega)$, $\alpha(\omega)$, and $L(\omega)$ of Bi-Sr-Ca-Cu-O are shown in Figs. 14 and 15, respectively. Substantial overall similarity to Y-Ba-Cu-O is noticeable.

V. DISCUSSION

A. In-plane plasmons in Y-Ba-Cu-O and Bi-Sr-Ca-Cu-O

In simple metals that show typical Drude behavior, bulk plasmons occur near $\tilde{\omega}_p = \omega_p / \sqrt{\epsilon_\infty}$; at that frequency, ϵ_1 has a zero, ϵ_2 is small, and $\mathrm{Im}(-1/\epsilon)$ has a sharp maximum. In the preceding section, we have shown that in high quality samples of Y-Ba-Cu-O and Bi-Sr-Ca-Cu-O all these traditional plasmon signatures are indeed found at about 1.4 and 1.1 eV, respectively. [This finding contradicts some earlier conclusions based on studies of pressed-powder samples.] Actually, it is fair to point out that the corresponding values of ϵ_2 are somewhat high (2–3), and the peaks of the loss function are relatively broad in both compounds; these facts are evidence of strong plasmon damping. The interpretation of this feature as an interband transition may be ruled out in view of the absence of the corresponding peak in ϵ_2, and even more because of the overall shape of that function. Hence we interpret the 1.1–1.4 eV feature as the in-plane-polarized plasmon. The preceding assignation is supported also by the available electron-energy-loss spectroscopy (EELS) data which are shown in the insets to Figs. 9 and 13; indeed, they match quite closely our calculated $\mathrm{Im}(-1/\epsilon)$.

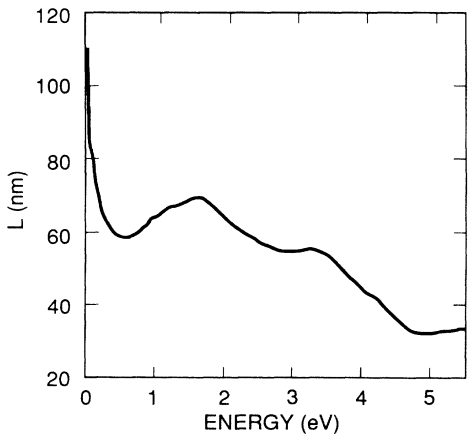

FIG. 11. The optical penetration depth of Y-Ba-Cu-O.

B. The value of ω_p

Using the approximate relation $\omega_p \approx \tilde{\omega}_p \sqrt{\epsilon_\infty}$, a crude estimate can be obtained for ω_p from the measured

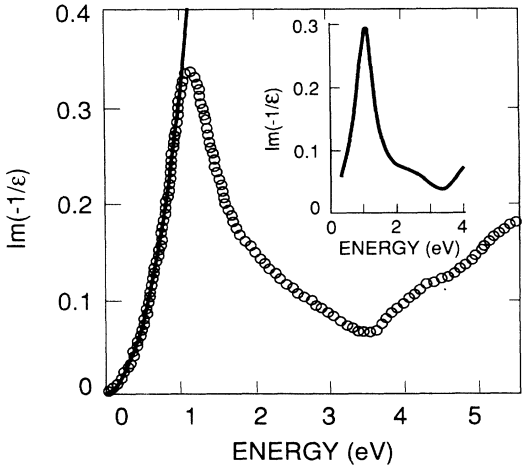

FIG. 13. The loss function of Bi-Sr-Ca-Cu-O derived in this work (open circles) and from EELS data (Ref. 50) (inset). The solid line is a square-law fit, $\mathrm{Im}(-1/\epsilon) = \beta\omega^2$, for $\hbar\omega \leq 1$ eV.

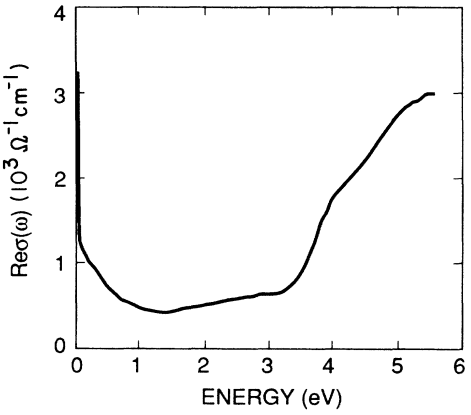

FIG. 14. The real part of the optical conductivity of Bi-Sr-Ca-Cu-O.

plasmon frequency. One gets $\hbar\omega_p \approx 3$ eV for Y-Ba-Cu-O and $\hbar\omega_p \approx 2.6$ eV in Bi-Sr-Ca-Cu-O. These estimates may be in error by 20% or so, partly because of the approximation itself and partly because of uncertainty in determining ϵ_∞.

An alternative, frequently utilized approach is to use the f-sum rule (7). However, as we have already pointed out in Sec. III A, the function Re $\sigma(\omega)$ is almost featureless [cf. Figs. 10 and 14], which makes separation of interband and intraband contributions ambiguous. On the other hand, it is comforting that several other independent experiments—transmittance, Resonant Raman scattering, ARPES, ellipsometry, etc.—have all shown[69] an interband transition onset close to about 2 eV in all HTSC cuprates. The same transition is seen in the insulating "parent" compounds; doping does not shift the frequency appreciably. Rather, the holes generated by doping reside in new, "impurity-like," in-gap states. Hence we attribute that additional, in-gap absorption to holes (polarons).[70] By integrating that absorption and using (7), we obtain $\hbar\omega_p = 3.2$ eV in Y-Ba-Cu-O and $\hbar\omega_p = 2.4$ eV in Bi-Sr-Ca-Cu-O (with about 10% error margin).

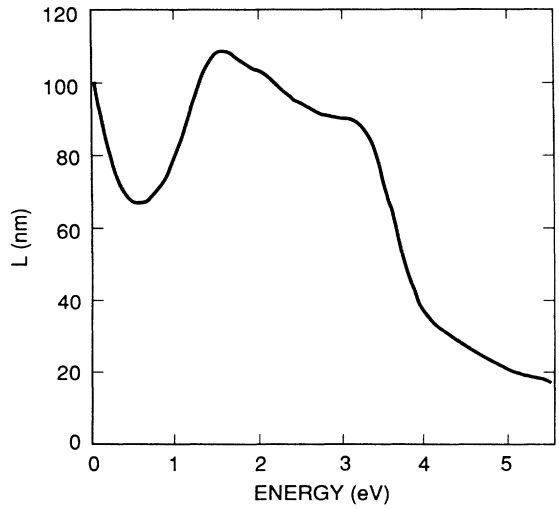

FIG. 15. The optical penetration depth of Bi-Sr-Ca-Cu-O.

Clearly, the preceding findings are not compatible with attempts to interpret the infrared absorption in cuprates by superimposing a Drude response on a mid-infrared exciton or interband transition, since in that way one arrives at much lower values of $\hbar\omega_p$. In Y-Ba-Cu-O, for example, it was inferred[15,16,23] that $\hbar\omega_p = 0.5-1.3$ eV; since $\epsilon_\infty \approx 4$, that corresponds to $\hbar\tilde{\omega}_p = 0.2-0.6$ eV, while we have found that $\hbar\tilde{\omega}_p = 1.4$ eV. As seen from Fig. 9, the EELS data unambiguously support the latter value.

In Bi-Sr-Ca-Cu-O, the situation is quite analogous. Our loss function gives $\hbar\tilde{\omega}_p = 1.1$ eV and it almost coincides with the one derived from the EELS (see Fig. 13), while the "excitonic" approach again provides 2–5 times lower values.

To further test our assertation that the strong infrared absorption comes, *grosso modo,* from the charge carriers, we plot

$$\Omega(\omega_1) = \left[8h^2 \int_0^{\omega_1} \mathrm{Re}\sigma(\omega)d\omega\right]^{1/2}$$

and

$$N(\omega_1) = \frac{2m_e}{\pi e^2} \int_0^{\omega_1} \mathrm{Re}\sigma(\omega)d\omega$$

as functions of the cutoff frequency ω_1, for Y-Ba-Cu-O in Fig. 16 and for Bi-Sr-Ca-Cu-O in Fig. 17. Because of the

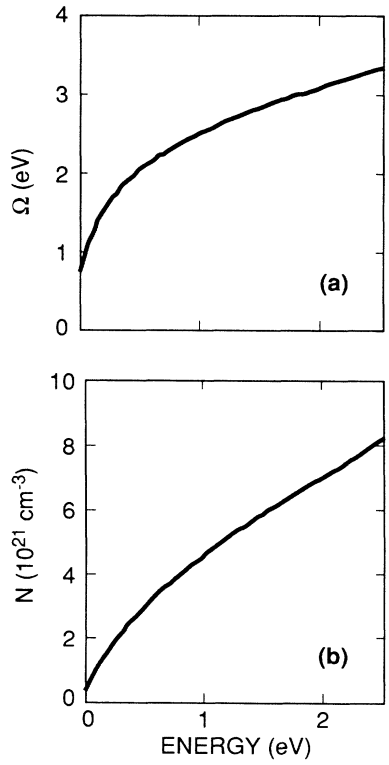

FIG. 16. The f-sum rule functions for Y-Ba-Cu-O:

(a) $\Omega(\omega_1) = \left[8h^2 \int_0^{\omega_1} \mathrm{Re}\sigma(\omega)d\omega\right]^{1/2}$

and

(b) $N(\omega_1) = (2m_e/\pi e^2) \int_0^{\omega_1} \mathrm{Re}\sigma(\omega)d\omega$.

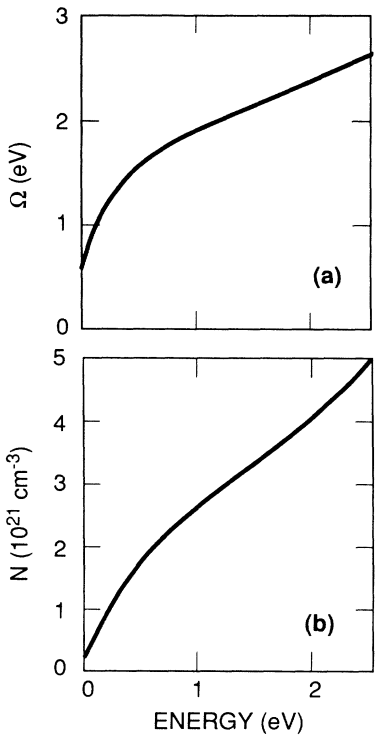

FIG. 17. The f-sum rule functions $\Omega(\omega_1)$ and $N(\omega_1)$ for Bi-Sr-Ca-Cu-O.

overlap of intraband and interband transitions, these functions are not horizontally sloped above the plasmon region, as would be the case for simple metals. Nevertheless, the range of concentrations of charge carriers that corresponds to the possible values of ω_p can be determined from Figs. 16 and 17. Assuming[71] that $m^*=m_e$ and $\hbar\omega_p=(3.2\pm0.3)$ eV, one gets $N=(7\pm1)\times10^{21}$ cm^{-1} in Y-Ba-Cu-O; in Bi-Sr-Ca-Cu-O where $\hbar\omega_p=(2.4\pm0.3)$ eV one gets $N=(4\pm1)\times10^{21}$ cm^{-3}. Certainly, these numbers are not too large; they are close to what one expects from stoichiometry, and what was inferred from Hall effect data,[57,72] namely $7-10\times10^{21}$ cm^{-3} in Y-Ba-Cu-O and $3-5\times10^{21}$ cm^{-3} in Bi-Sr-Ca-Cu-O. Hence we conclude that the oscillator strength in the infrared indeed comes from charge carriers—which, on the other hand, clearly do *not* behave like free electron gas.

In a way, the foregoing should have been obvious already from Fig. 4. Let us emphasize that no significant differences in chemical composition, crystallographic structure (as judged from x-ray diffraction patterns), etc. were detected between the films A and B; essentially, they differed only in oxygen content and thus in charge-carrier concentration.[73] Changing that concentration, apparently one can tune up or down the reflectance (and absorption) quite dramatically, all the way up to about 2 eV or so, and thus it seems natural to ascribe this absorption to charge carriers (holes).

C. Out-of-plane plasmons

So far we have assumed the direction of propagation of plasmons to be parallel to the CuO_2 layers. Experimental data pertinent to the perpendicular polarization are quite scarce. A major obstacle here is the lack of single crystals with smooth and large (say a few mm^2 at least) facets parallel to the c axis. In addition, to resolve clearly $R_\perp$ from $R_\parallel$ in such anisotropic materials (for example, $\rho_\perp/\rho_\parallel>100\,000$ in Bi-Sr-Ca-Cu-O!), the beam geometry (angle of incidence, beam divergence, etc.) must meet extremely strict requirements. In consequence, very little quantitative information about the out-of-plane (c-axis) plasmons in cuprates is available. Nevertheless, some qualitative statements can be made with confidence. In Y-Ba-Cu-O, there is a rise in $R_\perp(\omega)$ below 0.3–0.4 eV which resembles a plasma edge. However, $\omega_p^\perp$ is much lower[74] in Bi-Sr-Ca-Cu-O, lower than the typical phonon frequencies—if it can be defined at all. [The same is true for $La_{2-x}Sr_xCuO_4$, which also is more anisotropic than Y-Ba-Cu-O.] This we believe, rules out the possibility that plasmons which propagate along the "heavy" c axis could be the connecting thread of the HTSC phenomenon. Nevertheless, much more study is needed in this direction.

D. The nature of plasmons in Y-Ba-Cu-O and Bi-Sr-Ca-Cu-O: layered electron-gas behavior?

While studying the loss functions of Y-Ba-Cu-O and Bi-Sr-Ca-Cu-O, we have noticed a quite unusual feature: $\mathrm{Im}(-1/\epsilon)$ is almost perfectly—to within a percent or so—proportional to $(\hbar\omega)^2$ for $\hbar\omega<1$ eV, i.e., almost all the way up to the plasmon maximum. As seen from Figs. 7(a) and 7(b) and 10, this is true for both Y-Ba-Cu-O films A and B, as well as for Bi-Sr-Ca-Cu-O. In contrast, in ordinary metals one expects a Drude behavior:

$$\epsilon_1=\epsilon_\infty-\frac{\omega_p^2}{\omega^2+\Gamma^2},\quad \epsilon_2=\frac{\omega_p^2\Gamma}{\omega(\omega^2+\Gamma^2)} \tag{19}$$

so that

$$\mathrm{Im}(-1/\epsilon)=\frac{\epsilon_2}{\epsilon_1^2+\epsilon_2^2}=\frac{\omega(\omega^2+\Gamma^2)\omega_p^2\Gamma}{\omega_p^4\Gamma^2+\omega^2(\epsilon_\infty\omega^2+\epsilon_\infty\Gamma^2-\omega_p^2)^2}, \tag{20}$$

which for small ω behave like $(\Gamma/\omega_p^2)\omega+O(\omega^3)$. The best-fit Drude function (20) is also displayed in Fig. 9; apparently, it does not give the correct energy dependence. Rather, we believe that the $\mathrm{Im}(-1/\epsilon)=\beta\cdot\omega^2$ law, where β is a material-dependent constant, may be characteristic of another simple model, namely the layered electron-gas (LEG) model introduced in classic works of Fetter, Wischer and Falicov, Quinn and coworkers, and others.[75] It has a very characteristic plasmon spectrum, essentially different from that of an ordinary 3D metal: together with the usual optical plasmon branch, there are many (precisely, n_L-1, where n_L is the number of layers) acoustic plasmon branches as sketched in Fig. 18. If n_L is large, one could think of a cone filled with allowed plasmon states, so that indeed the total density of states should be proportional to energy squared. Hence one could expect to observe $\mathrm{Im}(-1/\epsilon)\propto(\text{energy loss})^2$ in EELS experiments in layered metal/semiconductor ma-

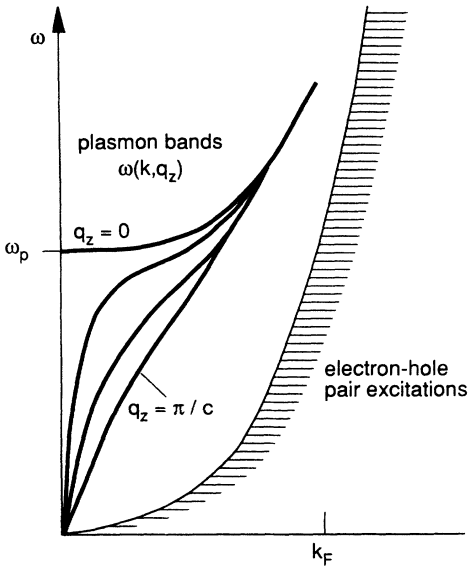

FIG. 18. The plasmon spectrum of LEG, after Ref. 8.

terials. As for the optical absorption, in ordinary metals and for visible or infrared light it is subject to the quasimomentum selection rule $\Delta k \approx 0$. If, however, there is some sort of quasilocalization (along the c axis) or substantial disorder on length scale much smaller than the photon wavelength—as indeed expected in our polaron picture—the $\Delta k_z \approx 0$ selection rule may be lifted, and for nearly normal incidence one could expect the EELS and the optical dielectric functions to coincide more or less. Indeed, that is what we see in Figs. 9 and 13. [A more rigorous theoretical treatment[76] of this issue arrived at the same conclusion—that the plasmon density of states of a LEG is proportional to ω^2, for small ω.]

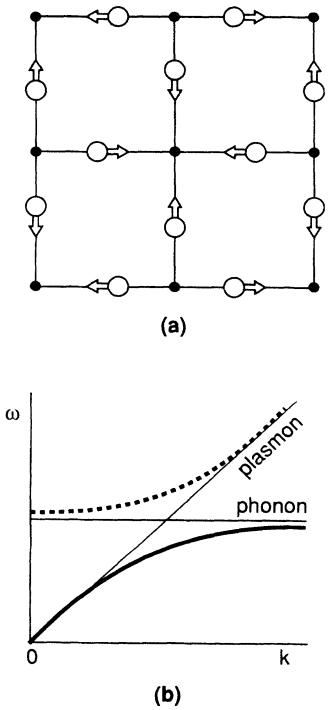

FIG. 19. (a) The oxygen breathing mode at $\mathbf{q}=(\pi/a,\pi/b,0)$. (b) Schematic representation of conceivable hybridization of such a vibration with an acoustic plasmon branch.

Hence we have discovered some evidence of the LEG-type behavior of the charge-carrier system in the normal state, in both Y-Ba-Cu-O and Bi-Sr-Ca-Cu-O. It may well be worth investigating further whether indeed this structure-related electronic property is one of the key prerequisites for the occurrence of the HTSC phenomenon. To begin with, the present analysis should be extended to other known HTSC materials; so far we did not have access to samples of other HTSC compounds of quality comparable to those referred to this study, but judging from the data available in the literature, the same seems to be true in $La_{2-x}Sr_xCuO_4$ single-crystalline films.[77] The next step may be to study the temperature dependence of the plasmon spectrum, as has been proposed recently.[78] Finally, one could look for some other indirect signatures of existence of acoustic plasmon branches. For example, they could interact strongly and hybridize with certain longitudinal optic phonon modes. Such hybridization—illustrated schematically in Fig. 19 for the oxygen breathing mode—should be detectable in the phonon spectrum, e.g., by inelastic neutron scattering.

VI. SUMMARY AND CONCLUDING REMARKS

In this paper, we have first tried to identify the principal sources of (large) uncertainty in previous determinations of spectral functions of HTSC compounds. Our attempts to reduce those errors have been described next. A novel method of deriving the real and the imaginary part of the dielectric function has been expounded, based on the analytic properties of that function and making use of reflectance and spectroellipsometric measurements on single crystals and epitaxial thin films. Using this method, we were able to determine the relevant spectral functions of Y-Ba-Cu-O and Bi-Sr-Ca-Cu-O within a few percent accuracy over a broad frequency range, from 5 meV to 6 eV. The present work thus complements the studies of Aspnes and Kelly,[56] extending into the potentially more interesting low-energy (mid- and far-infrared) region.

Our principal findings are the following. For in-plane polarization in Y-Ba-Cu-O, there is only one zero of $\epsilon_1(\omega)$, at about 1.4 eV in our best samples. The loss function $\mathrm{Im}(-1/\epsilon)$ has a pronounced maximum at the same energy. The same is true for Bi-Sr-Ca-Cu-O, except that the zero of ϵ_1 and the peak of $\mathrm{Im}(-1/\epsilon)$ occur at about 1.1 eV. We assign these features to in-plane free-carrier plasmons. Good agreement is found with recent EELS data, which clearly support the preceding assignment. The corresponding *bare* plasma frequencies are found to be $\hbar\omega_p=(3.2\pm0.3)$ eV in Y-Ba-Cu-O and $\hbar\omega_p=(2.4\pm0.3)$ eV in Bi-Sr-Ca-Cu-O. In both Y-Ba-Cu-O and Bi-Sr-Ca-Cu-O, we have found that $\mathrm{Im}(-1/\epsilon)=\beta\omega^2$. This law differs from Drude behavior; it may be compatible with the LEG model. We conjecture that it is universally obeyed in layered cuprate superconductors.

The preceding findings are in variance with models of HTSC which postulate the existence of low-energy exci-

tons or interband transitions that dominate the mid-infrared absorption, and Drude carriers with low plasma frequency. They also conflict with most of the plasmon-based models—for example, with those that require the existence of *d* mons or other similar low-frequency optic plasma branches. Insofar as the nature of the plasmons is concerned, the model of Kresin and Morawitz[8] seems to be the closest to our observation.

ACKNOWLEDGMENTS

The author is grateful to the Applied Physics Department, Stanford University, for hospitality; this paper is largely the final analysis of spectroscopic data he recorded there. Sincere thanks go to Professors T. Geballe, M. Beasley, and A. Kapitulnik for providing equipment, samples and support for this work. The high quality of the samples, mostly grown by K. Char and D. Mitzi, was particularly critical for success of the project. The same is true for the accuracy of the spectroellipsometric data of D. Aspnes and M. Kelly (Ref. 56), which in this work have been utilized as the calibration standard. Finally, inspiring discussions with all of those mentioned, as well as with H. Morawitz, V. Kresin, and D. Kirillov, are gratefully acknowledged.

[1]J. G. Bednorz and K. A. Muller, Z. Phys. B **64**, 189 (1986).

[2]*Novel Superconductivity,* edited by S. A. Wolf and V. Z. Kresin (Plenum, New York, 1987); Proceedings of the International Conference on High-Temperature Superconductivity and Materials and Mechanisms of Superconductivity, March 1988, Interlaken, Switzerland [Physica C **153-155**, (1988)].

[3]For general reviews, see J. G. Bednorz and K. A. Muller, Rev. Mod. Phys. **60**, 585 (1988); J. C. Phillips, *Physics of High-T_c Superconductors* (Academic, San Diego, 1989); C. P. Poole, Jr., T. Datta, and H. A. Farach, *Copper Oxide Superconductors* (Wiley, New York, 1989); T. H. Geballe and J. K. Hulm, Science **239**, 367 (1988); *Solid State Physics,* edited by H. Ehrenreich and D. Turnbull (Academic, Boston, 1989), Vol. 42. J. Talvachio [J. Low Temp. Phys. (to be published)] compiled a bibliography with 4600 entries on HTSC.

[4]I. Bozovic (unpublished); a brief account is presented in I. Bozovic, Physica C **162-164**, 1239 (1989).

[5]J. Ruvalds, Phys. Rev. B **35**, 8869 (1987).

[6]A. Griffin, Phys. Rev. B **37**, 5943 (1988).

[7]J. I. Gersten, Phys. Rev. B **37**, 1616 (1988).

[8]V. Z. Kresin and H. Morawitz, Phys. Rev. B **37**, 7854 (1988); J. Supercond. **1**, 89 (1988).

[9]J. Ashkenazi, C. G. Kuper, and R. Tyk, Physica B **148**, 366 (1987); Int. J. Mod. Phys. B **1**, 965 (1987); Solid State Commun. **63**, 1145 (1987).

[10]S. Perkowitz, G. L. Carr, B. Lou, S. S. Yom, R. Sudharsanan, and D. S. Ginley, Solid State Commun. **64**, 721 (1987).

[11]H. Krenn, G. Bauer, G. Vogl, G. Strasser, and E. Gornik, Phys. Rev. B **39**, 6716 (1989).

[12]J. R. Cooper, C. T. Chu, L. W. Zhou, B. Dunn, and G. Gruner, Phys. Rev. B **37**, 638 (1988).

[13]L. Genzel, A. Wittlin, J. Kuhl, H. Mattausch, W. Bauhofer, and A. Simon, Solid State Commun. **63**, 843 (1987).

[14]A. Porch, J. R. Waldram, and L. Cohen, J. Phys. F **18**, 1547 (1988).

[15]D. A. Bonn, A. H. O'Reilly, J. E. Greedan, C. V. Stager, T. Timusk, K. Kamaras, and D. B. Tanner, Phys. Rev. B **37**, 1574 (1988).

[16]T. Timusk, S. L. Herr, K. Kamaras, C. D. Porter, D. B. Tanner, D. A. Bonn, J. D. Garrett, C. V. Stager, J. E. Greedan, and M. Reedyk, Phys. Rev. B **38**, 6683 (1988).

[17]W. Markowitsch, W. Lang, N. S. Sariciftci, and G. Leising, Solid State Commun. **69**, 363 (1989).

[18]D. van der Marel, J. van Elst, G. A. Sawatzky, and D. Heitmann, Phys. Rev. B **37**, 5136 (1988).

[19]S. G. Barsov, A. L. Getalov, V. P. Koptev, L. A. Kuzmin, S. M. Mikirtych'yants, N. A. Tarasov, G. V. Shcherbakov, N. M. Kotov, A. S. Nigmatulin, Ya. M. Mukovskii, V. G. Grebinnik, V. N. Duginov, V. A. Zhukov, A. B. Lazarev, V. G. Ol'shevskii, S. N. Shilov, and E. D. Krasnoperov, JETP Lett. **46**, 499 (1989).

[20]J. Petzelt, S. Kamba, S. Pacesova, E. Pollert, J. Sramek, O. Smrckova, and D. Sykorova, Phys. Status Solidi B **146**, 743 (1988). The authors propose alternatively two plasma frequencies, 0.42 and 1.7 eV.

[21]T. Tanaka, K. Kamiya, M. Shimizu, M. Simada, C. Tanaka, H. Ozeki, K. Adachi, K. Iwahashi, F. Sato, A. Sawada, S. Iwata, H. Sakuma, and S. Uchiyama, Physica C **153-155**, 1752 (1988).

[22]D. W. Cooke, R. L. Hutson, R. S. Kwok, M. Maez, H. Rempp, M. E. Schillaci, J. L. Smith, J. O. Willis, R. L. Lichti, K. C. B. Chan, C. Boekema, S. P. Weathersby, J. A. Flint, and J. Ostens, Phys. Rev. B **37**, 9401 (1988).

[23]S. Mitra, J. H. Cho, W. C. Lee, D. C. Johnston, and V. G. Kogan, Phys. Rev. B **40**, 2674 (1989). Y-Ba-Cu-O powder was oriented in a magnetic field.

[24]Y. J. Uemura, J. Appl. Phys. **64**, 6087 (1988).

[25]T. Timusk, D. A. Bonn, J. E. Greedan, C. V. Stager, J. D. Garrett, A. H. O'Reilly, M. Reedyk, K. Kamaras, C. D. Porter, S. L. Herr, and D. B. Tanner, Physica C **153-155**, 1744 (1988).

[26]A. T. Fiory, A. F. Hebard, P. M. Mankiewich, and R. E. Howard, Phys. Rev. Lett. **61**, 1419 (1989).

[27]L. Krusin-Elbaum, R. L. Greene, F. Holtzberg, A. P. Malozemoff, and Y. Yeshurun, Phys. Rev. Lett. **62**, 217 (1989).

[28]Y. J. Uemura, V. J. Emery, A. R. Moodenbaugh, M. Suenaga, D. C. Johnston, A. J. Jacobson, J. T. Lewandowski, J. H. Brewer, R. F. Kiefl, S. R. Kreitzman, G. M. Luke, T. Riseman, G. E. Stronach, W. J. Kossler, J. R. Kempton, X. H. Yu, D. Opie, and H. E. Schone, Phys. Rev. B **38**, 909 (1988).

[29]D. R. Harshman, L. f. Scheemeyer, J. V. Waszczak, G. Aeppli, R. J. Cava, B. Batlogg, L. W. Rupp, E. J. Ansaldo, and D. L. Williams, Phys. Rev. B **39**, 851 (1989).

[30]D. R. Harshman, G. Aeppli, E. J. Ansaldo, B. Batlogg, J. H. Brewer, J. F. Carolan, R. J. Cava, M. Celio, A. C. D. Chaklader, W. N. Hardy, S. R. Kreitzman, G. M. Luke, D. R. Noakes, and M. Senba, Phys. Rev. B **36**, 2386 (1987).

[31]W. Ose, P. E. Obermayer, H. H. Otto, T. Zetterer, H. Lengfellner, J. Keller, and K. F. Renk, Z. Phys. B **70**, 307 (1988).

[32]T. W. Noh, P. E. Sulewski, and A. J. Sievers, Phys. Rev. B **36**, 8866 (1987).

[33]P. E. Sulewski, T. W. Noh, J. T. McWhirter, A. J. Sievers, S. E. Russek, R. A. Buhrman, C. S. Jee, J. W. Crow, R. E. Salo-

mon, and G. Myer, Phys. Rev. B **36**, 2357 (1987).

[34]I. Bozovic, D. Kirillov, A. Kapitulnik, K. Char, M. R. Hahn, M. R. Beasley, T. H. Geballe, Y. H. Kim, and A. J. Heeger, Phys. Rev. Lett. **59**, 2219 (1987).

[35]Z. Schlesinger, R. T. Collins, D. L. Kaiser, F. Holtzberg, G. V. Chandrasekhar, M. W. Shafer, and T. M. Plaskett, Physica C **153-155**, 1734 (1988).

[36]R. T. Collins, Z. Schlesinger, F. Holtzberg, P. Chaudhari, and C. Feild, Phys. Rev. B **39**, 6571 (1989).

[37]C. Tarrio and S. E. Schnatterly, Phys. Rev. B **38**, 921 (1988).

[38]J. Orenstein, G. A. Thomas, D. H. Rapkine, C. G. Bethea, B. F. Levine, R. J. Cava, E. A. Rietman, and D. W. Johnson, Jr., Phys. Rev. B **36**, 729 (1987).

[39]S. Tajima, T. Nakahashi, S. Uchida, and S. Tanaka, Physica C **156**, 90 (1988). The authors actually reported $\hbar\tilde{\omega}_p = 1.25$ eV. For consistency, in Table I we entered $\hbar\omega_p = 3.1$; that value is obtained for $\epsilon_\infty = 4$ and $\hbar\Gamma = 0.9$ eV.

[40]Z. Schlesinger, R. T. Collins, D. L. Kaiser, and F. Holzberg, Phys. Rev. Lett. **59**, 1958 (1987); Z. Schlesinger, R. T. Collins, M. W. Shafer, and E. M. Engler, Phys. Rev. B **36**, 5275 (1987).

[41]G. A. Thomas, J. Orenstein, D. H. Rapkine, M. Capizzi, A. J. Millis, R. N. Bhatt, L. F. Schneemeyer, and J. V. Waszczak, Phys. Rev. Lett. **61**, 1313 (1989). The authors also propose $\hbar\omega_p = 1$ eV. The Y-Ba-Cu-O crystals had reduced $T_c = 50$–70 K.

[42]A. Bjorneklett, A. Borg, O. Hunderi, and S. Julsrud, Solid State Commun. **67**, 525 (1988).

[43]R. Felici, J. Penfold, R. C. Ward, E. Olsi, and C. Matacotta, Nature **329**, 523 (1987).

[44]Y. Chang, M. Oneilion, D. W. Niles, R. Joynt, G. Margaritondo, N. G. Stoffel, and J. M. Tarascon, Solid State Commun. **63**, 714 (1987). The authors assign the 17 eV feature to surface plasmons and the 25 eV feature to volume plasmons.

[45]Y. Chang, Y. Hwu, M. Oneillion, G. Margaritondo, P. A. Morris, and W. A. Bonner, Phys. Rev. B **38**, 4996 (1988). The 20 eV feature was attributed to surface plasmons and the 25 eV feature to volume plasmons.

[46]A. Ando, K. Saiki, K. Ueno, and A. Koma, Jpn. J. Appl. Phys. **27**, L304 (1988); A. Balzarotti, M. De Crescenzi, N. Motta, F. Patella, and A. Sgarlata, Solid State Commun. **68**, 381 (1988).

[47]I. Bozovic, K. Char, S. J. B. Yoo, A. Kapitulnik, M. R. Beasley, T. H. Geballe, Z. Z. Wang, S. Hagen, N. P. Ong, D. E. Aspnes, and M. K. Kelly, Phys. Rev. B **38**, 5077 (1988).

[48]O. V. Kosogov, M. V. Belousov, V. A. Vasilev, V. Yu Davidov, K. G. Dyo, A. A. Kopylov, V. D. Petrikov, and V. V. Tretyakov, JETP Lett. **48**, 530 (1989).

[49]M. Reedyk, D. A. Bonn, J. D. Garrett, J. E. Greedan, C. V. Stager, T. Timusk, K. Kamaras, and D. B. Tanner, Phys. Rev. B **38**, 11 981 (1988).

[50]N. Nucker, H. Romberg, S. Nakai, B. Scheerer, J. Fink, Y. F. Yan, and Z. X. Zhao, Phys. Rev. B **39**, 12379 (1989). The authors actually reported $\hbar\tilde{\omega}_p = 1.0$ eV and $\epsilon_\infty = 4.5$. As for Ref. 33, we listed in Table II $\hbar\omega_p = 2.85$ eV, calculated assuming $\hbar\Gamma = 0.9$ eV.

[51]K. Char, M. R. Hahn, T. Hylton, M. R. Beasley, T. H. Geballe, and A. Kapitulnik, IEEE Trans. Magn. **MAG-25**, 2422 (1989); A. Kapitulnik and K. Char, IBM J. Res. Dev. **33**, 252 (1989); K. Char, A. Kapitulnik, and I. Bozovic (unpublished).

[52]Z. Z. Wang, B. Y. Lin, A. Kahn, and N. P. Ong, Bull. Am. Phys. Soc. **34**, 423 (1988); Y. Watanabe, Z. Z. Wang, S. A. Lyon, D. C. Tsui, N. P. Ong, J. M. Tarascon, and P. Barboux, Phys. Rev. B **40**, 6884 (1989).

[53]K. Char, M. Lee, R. W. Barton, A. F. Marshall, I. Bozovic, R. H. Hammond, M. R. Beasley, T. H. Geballe, and A. Kapitulnik, Phys. Rev. B **38**, 834 (1988).

[54]H. P. Geserich, G. Scheiber, J. Geerk, H. C. Li, G. Linker, W. Assmus, and W. Weber, Europhys. Lett. **6**, 277 (1988); H. P. Geserich, B. Koch, G. Scheiber, J. Geerk, H. C. Li, G. Linker, W. Weber, and W. Assmus, Physica C **153-155**, 661 (1988).

[55]K. C. Hass, in *Solid State Physics,* edited by H. Ehrenreich and D. Turnbull (Academic, Boston, 1989), Vol. 42, p. 213.

[56]M. K. Kelly, P. Barboux, J-M. Tarascon, D. E. Aspnes, W. A. Bonner, and P. A. Morris, Phys. Rev. B **38**, 870 (1988); D. E. Aspnes and M. K. Kelly, Int. J. Quantum Electron. (to be published); M. K. Kelly, P. Barboux, J-M. Tarascon, and D. E. Aspnes (unpublished).

[57]D. B. Mitzi, L. W. Lombardo, A. Kapitulnik, S. S. Laderman, and R. D. Jacowitz, Phys. Rev. B **41**, 6564 (1990).

[58]M. D. Kirk, J. Nogami, E. E. Baski, D. B. Mitzi, A. Kapitulnik, T. H. Geballe, and C. F. Quate, Science **242**, 1673 (1988).

[59]S. Tajima, T. Nakahashi, S. Uchida, and S. Tanaka, Physica C **156**, 90 (1988); S. Uchida, S. Tajima, H. Takagi, and Y. Tokura, in *Mechanisms of High-Temperature Superconductivity,* edited by H. Kamimura and A. Oshiyama (Springer, Berlin, 1989), p. 197.

[60]T. Timusk and D. B. Tanner, in *Physical Properties of High Temperature Superconductors,* edited by D. M. Ginsberg (World Scientific, Singapore, 1989).

[61]Polaron signatures in the infrared absorption spectra had been elucidated in the classic works of Eagles, Reik, Bogomolov, and Firsov; see, e.g., D. M. Eagles, Phys. Rev. **130**, 1381 (1963); **145**, 645 (1966); J. Phys. Chem. Solids **25**, 1243 (1964); H. G. Reik, Z. Phys. **203**, 346 (1967); J. Phys. Chem. Solids **28**, 581 (1967); V. N. Bogomolov, E. K. Kudinov, D. N. Mirlin, and Y. A. Firsov, Sov. Phys. Solid State **9**, 1630, 2502 (1968); Y. A. Firsov, *ibid.* **10**, 1950 (1968); V. N. Bogomolov and D. N. Mirlin, Phys. Status Solidi **27**, 443 (1968). For a general introduction to polarons, see J. Appel, in *Solid State Physics,* edited by F. Seitz, H. Ehrenreich, and D. Turnbull (Academic, Boston, 1968), Vol. 42, p. 193; I. G. Austin and N. F. Mott, Adv. Phys. **18**, 41 (1969); *Polarons,* edited by Y. A. Firsov (Nauka, Moscow, 1975) (in Russian); M. K. Klinger, *Problems of Linear Electron (Polaron) Transport Theory in Semiconductors* (Pergamon, New York, 1979).

[62]F. Abeles, in *Progress in Optics,* edited by W. Wolf (North-Holland, Amsterdam, 1963), Vol. 2.

[63]D. E. Aspnes, in *Handbook of Optical Constants of Solids,* edited by E. Palik (Academic, Boston, 1985), Chap. 5.

[64]J. Humlicek, M. Garriga, M. Cardona, B. Gegenheimer, P. Berberich, and J. Tate, Solid State Commun. **66**, 1071 (1988).

[65]B. Velicky, Czech. J. Phys. B **11**, 787 (1961).

[66]Similar ideas had indeed appeared recurrently in the literature and can be traced back to early works of Velicky (Ref. 65) and Miloslavskii [Opt. Spectrosc. **21**, 193 (1966)]. However, they used only one ellipsometric data point and only the first term in (20); that considerably reduces the accuracy of the method, which never gained popularity.

[67]Actually, this should not even be surprising; see Ref. 16 for an earlier careful comparative assessment of different optical methods in which the same conclusion was reached—even in the cases when reflectance was measured over much wider frequencies.

[68]A strong, narrow excitonic peak does appear, at 4.1 eV, in oxygen-depleted insulating samples. However, it disappears after oxygen annealing (see Refs. 56 and 64), which, we be-

lieve, signifies that screening increases as the carriers are added, so that eventually excitons are "dissolved," i.e., they do not form in the metallic phase. An excitonic mechanism for HTSC thus seems rather unlikely, as stated in Ref. 34.

[69]D. Kirillov, I. Bozovic, K. Char, and A. Kapitulnik, J. Appl. Phys. **66**, 977 (1989); T. Takahashi (unpublished); G. Wendin, Phys. Scr. T **27**, 31 (1989).

[70]In the sequel, see Ref. 4, we will try to show that the polaronic model (see Ref. 61) provides a quantitatively accurate description of frequency, temperature, and carrier concentration dependence of spectral functions. The model also explains why the values of ω_p derived from muon spin resonance data (via the relation $\omega_p = c/\lambda_L$, and using the measured penetration depth) or from magnetization measurements are unrealistically small; these low-frequency probes sense the heavy mass of "dressed" polarons. Optical spectroscopy and EELS, in contrast, probe the relevant frequency region close to the actual plasmon frequency.

[71]The actual values of the optical effective mass in Y-Ba-Cu-O and Bi-Sr-Ca-Cu-O may be somewhat different; they have to be determined from independent experiments.

[72]Z. Z. Wang, J. Clayhold, N. P. Ong, J-M. Tarascon, L. H. Greene, W. R. McKinnon, and G. W. Hull, Phys. Rev. B **36**, 7222 (1987); G. S. Grader, P. K. Gallagher, and A. T. Fiory, Phys. Rev. Lett. **38**, 844 (1988); J. Clayhold, N. P. Ong, P. H. Hor, and C. W. Chu, Phys. Rev. B **38**, 7016 (1988); Y. Koike, Y. Iwabuchi, and S. Hosoya, Physica C (to be published).

[73]So far, we were not able to determine quantitatively the oxygen content in thin films. (The task is indeed demanding—it amounts to measuring mass variations to better than 10^{-9} g accuracy.) Our qualitative statement is based on the studies of transport properties (conductivity, Hall effect) and Raman scattering by Dr. K. Char at Stanford and Dr. D. Kirillov at Varian, respectively. [The frequencies and the intensities of certain Raman bands scale with oxygen concentration. See, e.g., G. A. Kourouklis, A. Yayaraman, B. Batlogg, R. J. Cava, M. Stavola, D. M. Krol, E. A. Rietmann, and L. F. Schneemayer, Phys. Rev. B **36**, 8320 (1987); D. Kirillov, J. P. Collman, J. T. McDevitt, G. T. Yee, M. J. Holcomb, and I. Bozovic, *ibid.* **37**, 3660 (1988); R. M. Macfarlane, H. J. Rosen, E. M. Engler, R. D. Jacowitz, and V. Y. Lee, *ibid.* **38**, 284 (1988); C. Thomsen, M. Cardona, K. Kres, R. Liu, L. Genzel, M. Bauer, E. Schoenherr, and U. Schroeder, Solid State Commun. **65**, 1139 (1988).] Furthermore, one can shift the "plasma edge" up (down), reversibly, by annealing in oxygen (nitrogen), and moreover the shifts correlate well with the Hall number variations; see, e.g., N. Bontemps, D. Fournier, A. C. Boccara, P. Monod, H. Alloul, J. Arabski, P. Regnier, and G. Deutcher, Physica C **162-164**, 1113 (1989), and Refs. 39 and 59.

[74]Y. Kim, I. Bozovic, D. Mitzi, A. Kapitulnik, and J. Harris, Phys. Rev. B **41**, 7251 (1990).

[75]P. B. Visscher and L. M. Falicov, Phys. Rev. B **3**, 2541 (1971); A. L. Fetter, Ann. Phys. (N.Y.) **88**, 1 (1974); S. Das Sarma and J. J. Quinn, Phys. Rev. B **25**, 7603 (1982); A. C. Tselis and J. J. Quinn, *ibid.* **29**, 3318 (1984).

[76]H. Morawitz, I. Bozovic, and V. Z. Kresin (unpublished).

[77]T. Tanaka, K. Kamiya, M. Shimizu, M. Simada, C. Tanaka, H. Ozeki, K. Adachi, K. Iwahashi, F. Sato, A. Sawada, S. Iwata, H. Sakuma, and S. Uchiyama, Physica C **153-155**, 1752 (1988).

[78]V. Z. Kresin and H. Morawitz, in *Studies of High Temperature Superconductors,* edited by A. Narlikar (Nova Science, Commack, 1989), Vol. 2, p. 305.